

Use of carbonized corn cob biomass to reduce acidity of residual frying oil

Aline Bavaresco^{1*}, Jhessica Marchini Fonseca², Fabiano Bisinella Scheufele³, Camila da Silva^{2,4} and Joel Gustavo Teleken^{1,5}

¹Programa de Pós-Graduação em Bioenergia, Universidade Federal do Paraná, Rua Pioneiro, 2153, 85950-000, Palotina, Paraná, Brazil. ²Programa de Pós-Graduação em Bioenergia, Universidade Estadual do Maringá, Maringá, Paraná, Brazil. ³Programa de Graduação em Engenharia de Bioprocessos e Biotecnologia, Universidade Tecnológica Federal do Paraná, Toledo, Paraná, Brazil. ⁴Departamento de Tecnologia, Universidade Estadual de Maringá, Umuarama, Paraná, Brazil. ⁵Departamento de Engenharias e Ciências Exatas, Universidade Federal do Paraná, Palotina, Paraná, Brazil. *Author for correspondence. E-mail: aline.bava@gmail.com

ABSTRACT. The objective of this work was to evaluate the ability of CCC as an adsorbent material for the acidity removal of RFO, aiming at the application of the oil in biodiesel production. For that, a RCCD was used for FFA removal by applying the CCC and CAC for comparative purposes. In the RCCD removal assays the effect of the Temperature, Agitation and Mass factors were assessed over acidity removal of the oil. Under the best conditions from RCCD, an evaluation of adsorption kinetics was performed, wherein it was observed the equilibrium was reached within 4 h, for the CCC. Also, the influence of the adsorbent dosage was performed. It was verified that 4 g was sufficient to allow the system to reach the maximum FFA removal. Overall, the CCC presented results approximately twice as high than those obtained by the CAC, mainly due to the pore size distribution which led to a “molecular sieving effect” for the CCC adsorbent. It allowed the major diffusion of the FFA molecules inside its narrow-distributed pores, whereas the CAC with a wider pore distribution (up to 260 Å) resulted in the larger molecules competition for the active sites inside the porous structure. The adsorbents’ characterization also evidenced that CCC adsorbent presented a higher content of oxygenated groups in its surface which acted as potential active sites for the FFA molecules resulting in an enhanced adsorbent-adsorbate affinity. Lastly, the wastes generated in the adsorption experiments, were evaluated as to their calorific power resulting in a value of 31,933 J g⁻¹, suggesting that it could be further used for energetic purposes, such as a solid fuel for boilers and furnaces to generate thermal energy. Based on these results, the CCC stands out as a promising material for RFO acidity removal.

Keywords: adsorption; activated carbon; free fatty acids; oil acidity.

Received on December 5, 2019.

Accepted on April 15, 2020.

Introduction

The use of waste vegetable oil originated from the frying food process as a fatty material source for biodiesel production can significantly reduce the cost, besides being considered an important step for the waste minimization and recycling. Its physical and chemical characteristics are closely associated with the presence of contaminants such as water, derived from the food and free fatty acids processing (FFA), as well as dimers and polymers that directly influence the transesterification reaction (Diya’uddeen, Albul Aziz, Daud, & Chakrabarti, 2012; Fonseca et al., 2019 ; Rocha Junior et al., 2019; Vieitez et al., 2014).

The acidity index determination (AI) can provide an important element in the assessment of the oil conservation status, including the assessment of the amount of residual fatty acids which have not undergone oxidation (Silva, Borges, & Ferreira, 1998; Xia & Budge, 2017). Thus, a pre-treatment of the raw material, should aim better reaction yields and better product quality, acting physically in the removal of any suspended solids and contaminants, and chemically, deacidifying the medium (Berrios & Skelton, 2008; Maddikeri, Pandit, & Gogate, 2012; Casallas et al., 2018).

To remove such compounds, the most commonly used processes are washing with hot water, neutralization with bases, steam injection, centrifuging and adsorption. Most of these processes require high temperature or large quantities of solvents, making them unfeasible due to the high operational cost (Nascimento, Lima, Vidal, Melo, & Raulino, 2014; Talebian-Kiakalaieh, Amin, & Mazaheri, 2013). The use of adsorbent materials has been conquering space and importance in the purification steps of vegetable oil, for

their efficiency and low energy costs when several types of synthetic adsorbents are usually used, such as activated carbons (Cai et al., 2015; Ullah, Bustam, & Man, 2015; Yaakob, Mohammad, Alherbawi, Alam, & Sopian, 2013). Recently, several organic materials considered as waste from the agricultural sector of crops such as soybeans, corn, wheat or sugar cane, have been tested and recognized as adsorbents for the purification process of frying residual oil as well as biodiesel (Bonassa et al., 2016; Fonseca et al., 2018; Manique, Faccini, Onorevoli, Benvenuti, & Caramão, 2012).

Ashes from sugar cane bagasse were investigated in the removal of several compounds present in the residual sunflower oil, among them free fatty acids (Ali & El Anany, 2014). Ashes from sugarcane bagasse were also investigated for the removal of free fatty acids from residual frying oil, evaluating different operational variables in the adsorption process (Bonassa et al., 2016). Rice husks were also used in the removal of free fatty acids from waste oil (Schneider et al., 2017) as well as sugarcane bagasse used in the purification of residual frying oil (Miyashiro et al., 2018). Biodiesel produced from frying waste oil was purified from rice husks to remove free fatty acids, water, among others (Fonseca et al., 2018).

In 2017 the world corn production exceeded 1 billion tons (Food and Agriculture Organization of the United Nations [FAO], 2017), Brazil is responsible for almost 100 million tons. Corn is an important raw material for glucose, starch, oil and a rich source of nutrients (Ozturk & Esen, 2013).

The ear of corn is the main part of the plant, which is formed by the peel and straw, cob and grains. The ear is known by the inflorescence which has an axis, known as the cob, surrounded by flowers that come loose easily, originating the grains. The ear is composed of 70 % of grain, 20 % of cob and 10 % of straw. Therefore, each 100 kg of ears, generates 20 kg of cob (Silvério et al., 2013; Texeira, 1998). The cob of corn stands out by its high production volume and its low associated costs since it is an agricultural by-product, usually underused (Vaughan, Seo, & Marshall, 2001) and composed of cellulose (38 %), hemicellulose (36 %) lignin (13 %) and ash (3 %) (Liu et al., 2010).

Based on the above, the objective of this work was to obtain a carbonized material of corn cobs, an abundant agricultural waste in Brazil, and apply it in the waste oil pre-treatment intended for the biodiesel production. The carbonaceous material was characterized and used as an adsorbent for removal of free fatty acids, which evaluated the effect of operational variables, as well as the adsorption kinetics and the mass of the adsorbent effect. A computational simulation of the size of the fatty acid molecules present in the residual oil was performed in order to investigate the access to the pores of the adsorbent material. In parallel, experiments were conducted using commercial activated carbon (CAC) for comparative purposes.

Material and methods

Obtaining and characterization of materials

The in natura corn cob (CC) and the residual frying oil (RFO) used in the study were purchased in the region of Palotina, Paraná State, Brazil. The commercial activated carbon (CAC), used as a reference for the experiments, with uniform particle size of 0.004 mm (4 µm), was supplied by Alphatec. Figure 1 presents the preparation and/or treatment steps of each material used. Both adsorbents and the frying residual oil were characterized by the methods described in Table 1.

Table 1. Techniques for the characterization of materials.

Tests	Application	Reference
Nitrogen Physisorption (B.E.T. method)	CC, CCC and CAC	Gregg and Sing (1982)
Scanning Electron Microscopy (SEM)	CC, CCC and CAC	Moruzzi, Lima, Colombo, Conceição and Lanza (2014); Souza, Matsushita and Visentainer (2012)
Energy- Dispersive X-ray Spectrometry (EDS) – Coupled to SEM	CC, CCC and CAC	Moruzzi et al. (2014); Souza et al. (2012)
Infrared Spectroscopy (FT-IR)	CC, CCC, CAC, RFO, RFOT and adsorbents impregnated with RFO	Pavia, Lampman, Kris and Vyvyan (2010)
pH _{PCZ}	CCC and CAC	Freitas, Câmara and Martins (2015)
Acidity Index (AI)	RFO and RFO	American Oil Chemists' Society (2009)
Fatty acids composition	RFO	European Committee for Standardization (2003)

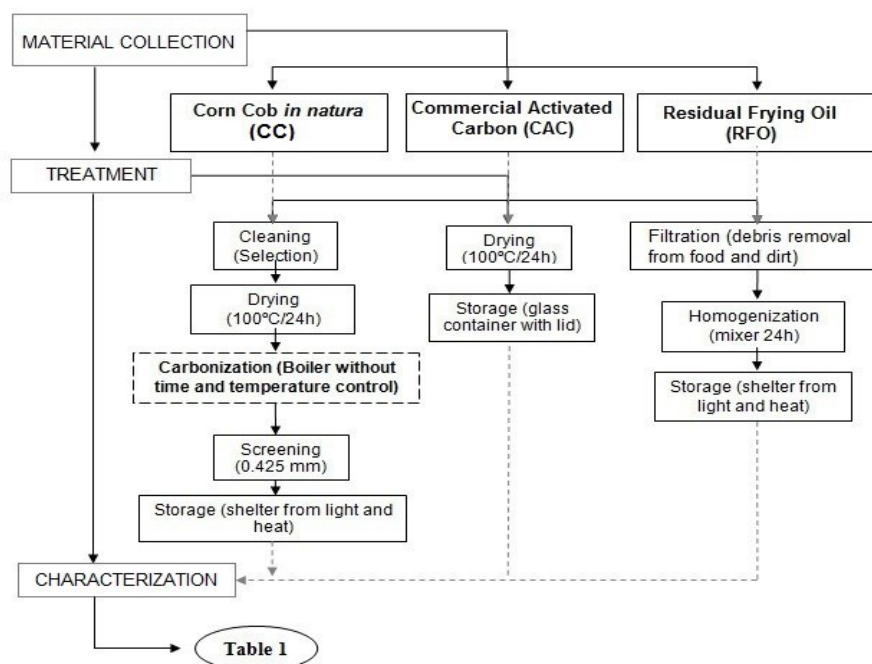


Figure 1. Flow chart of the procedure of material collection, and preparation of the adsorbents.

Computational simulation of fatty acids molecular diameter

Two computational theoretical tests were performed in order to predict the size of the fatty acid molecules present in the frying residual oil and assess the possibility of their diffusion into the pores of the studied adsorbents.

Initially, the molecular geometry of fatty acids present in the RFO was estimated by the minimizing energy MMFF94 method simulated in the JSmol (3D rendering engine – Mol View software v. 2.4). This method provided the medium and longitudinal diameters of each molecule found in fatty acid composition, without, however, considering the interference of electronic cloud present in the molecules.

Next, the oleic acid molecule simulation acid was performed, specifically, for being the second most abundant in the analysed RFO sample, and easily purchased. This simulation was carried out by means of the computational method of HARTREE-FOCK (HF), a semi-empirical AM2 method, which includes data from classical calculations and quantum mechanics. In this case, a computer with Linux operating system Ubuntu, i7 processor of 3.40 MHz and 8.0 GB of RAM memory was used. The software used for the input generation was Gabedit 4.2.8, for processing it was the Gaussian 03®, and for output and data processing was Gaussview 4.1®. Through this method, it was possible to consider all the electronic clouds interference and, therefore, all the space occupied by them.

Adsorption tests

For the removal tests with adsorbent materials (see Figure S1 - Supplementary Material) whose goal was to reduce the RFO acidity, a water bath Dubnoff was used (New Instruments, NI-1232 model), with temperature control and agitation. An experimental design based on a Rotational Central Composite Design (RCCD) was developed proposed for each of the adsorbents. The purpose was the adsorption process optimization by reducing the number of tests, where it was assessed the effect of the operational variables (X_1 – Temperature (T), X_2 – Adsorbent Mass (M) and X_3 – Agitation (A)) over the response variable (Y – Acidity Reduction of RFO – RA) by means of Analysis of Variance (ANOVA) and Response Surface Methodology (RSM). The specification of the operational variables of the RCCD are presented in Table S1 (see Supplementary Material).

RCCD used the contemplated 3 (three) factors in 5 (five) levels, providing a factorial design type 2^3 with 6 axial points and triplicate in the central point, totalling 17 assays (see Table S2). The choice of the values of each of the independent variables was accomplished taking into consideration the technical capacity of the available equipment to perform the tests.

The data obtained in the Acidity Index analysis (AI) were interpreted as the percentage of reduction of Acidity Reduction (RA %) when compared with the initial acidity content of frying residual oil. The tests were performed in analytics triplicate. These data were statistically evaluated with the aid of the Statistica v. 7.0.

Adsorption kinetics and evaluation of the adsorbent mass

Based on the maximum value of RA (%) obtained, a study of the adsorption kinetics was performed, being values of Temperature (T), Agitation (A) and Adsorbent Mass (M) kept fixed, known in optimal condition. An evaluation at different times of assay was performed (15 min, 30 min, 1 min, 2 min, 3 min, 4 min, 5 min, 6 min, 7 min, 8h and 9h). The purpose of this procedure was to verify the contact time required between adsorbent and adsorbate, to observe the highest RA (%) (*i.e.* the equilibrium time).

From the definition of the time of maximum removal of FFA through the adsorption kinetics study, a verification was carried out on the influence the mass of adsorbent variation would play in this process, aiming to find out the best values of RA (%) of free fatty acids present in the frying residual oil. In this case, values of temperature and agitation of optimal condition observed were maintained, wherein it was evaluated only the mass of adsorbent used for the tests, starting with 1 g to 10 g of adsorbent, gradually increasing in 1 g. The oil mass was maintained at 33 g.

Results and discussion

Materials Characterization

The N₂ physisorption analysis, performed by the BET (Brunauer, Emmett, Teller) method allowed to know the superficial area values of each adsorbent material, and through the BJH method, the values of volume and pore size distribution were determined (see Table 2 and Figure S2)

Table 2. Textural characteristics of in natura corn cobs and the adsorbents analyzed by the N₂ physisorption method.

Samples	S _{BET} (m ² g ⁻¹)	S _m (m ² g ⁻¹)	V _T (cm ³ g ⁻¹)	V _m (cm ³ g ⁻¹)	Ø _p (Å)	Classification
CC	2.662	-	0.006557	0.0002164	98.50	Mesopores
CCC	109.380	140.7	0.07522	0.04999	27.50	Mesopores
CAC	564.400	819.8	0.3564	0.2913	25.26	Mesopores

Specific surface area (S_{BET}); Micropore Area (S_m) (a total of these two items equivalent to the total surface area); Total pore volume (V_T); Micropore volume (V_m); Average pore diameter (Ø_p).

Higher specific surface area and larger volume of pores were observed for the commercial activated carbon (CAC), a fact that may be related to the differentiated conditions of this sample production, since it is a commercial activated carbon, unlike other samples that have not gone through any type of activation. Usually, the activated carbons show a high surface area, reaching 2400 m² g⁻¹ (Gupta & Suhas, 2009). Their volume of pores also tends to be high, approximately 0.60 cm³ g⁻¹ (Lopez et al., 2013). Thus, regarding to the micropores, their volume and surface area were also higher than the other samples. However, comparing the CC with the CCC, it is noted that the carbonization process applied to corn cobs let to an increase of all the parameters shown in Table 2.

In CCC (see Figure S2) one may notice that the macropores volume is negligible in contrast to the CC, which presented macropores within the range of 170 to 800 Å (or higher). This behaviour is related to the carbonization process in which a mesoporous structure started increasing, consequently, the pore volume and the surface area of the CCC, as presented in Table 2. Analysing the pore size distribution of the CCC (Figure S2) one may notice the predominance of mesopores of homogeneous size concentrated in a narrow range, where its distribution showed a more acute frequency curve, and also a tendency for micropores, which is in accordance with the micropores area values observed for the CC (Table 2). The pore size distribution obtained for the CCC stands out as a major feature for the adsorbent, since it can provide selectivity for the adsorbent on the removal of fatty acids molecules, selecting those with diameters smaller than those of the adsorbent, rather than larger molecules.

Regarding the CAC adsorbent, larger pore volumes are observed, mainly concentrated in the range from 30 to 50 Å, however in minor quantity up to 120 Å (mesopores). There is also a tendency, more expressive, for micropores and a smaller volume of macropores. Thus, one may suggest that larger molecules are adsorbed easier in CAC than in CCC.

The micrographs obtained by SEM (Figure 2) indicated that the CC had clustered thin tubular structures (a), containing some small visible pores and long and fibrous structures (b). Whereas in the CCC micrographs (a and b) a greater quantity of scattered pores throughout the structure is observed that seems to take shape of rings. In CAC, a more defined structure was observed.

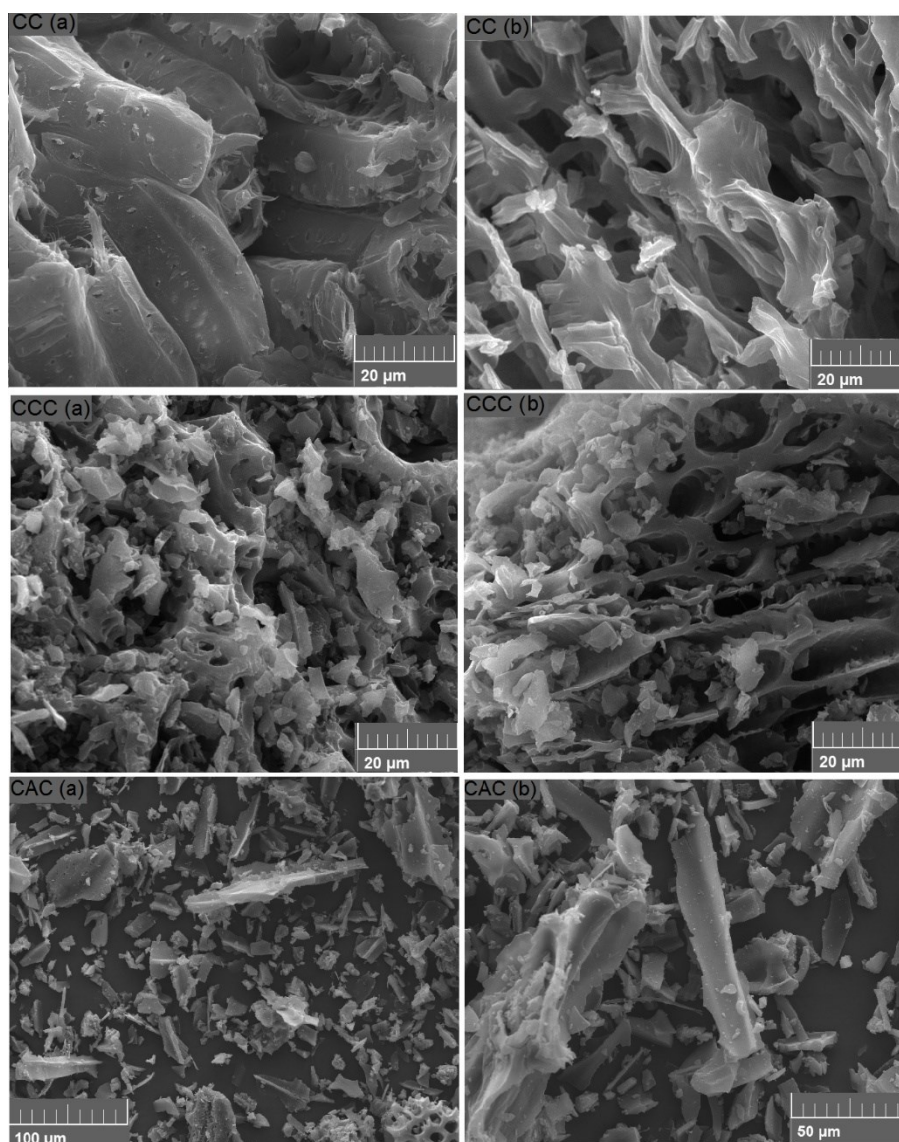


Figure 2. Micrographs of in natura corn cobs– CC (a and b, 30.0 kV, 2.00 kx); Carbonized Corn Cobs – CCC (a and b, 30.0 kV, 2.00 kx) and Commercial Activated Carbon – CAC (a - 20 kV, 500x and b - 20 kV, 1.0 kx).

Through the Energy-Dispersive X-ray Spectroscopy (EDS) analysis (Table 3) it was noticed that the corn cobs in natura exhibited a considerably higher quantity of carbon, which implies to be a potential raw material for the activated carbon production. The quantity of this chemical element in a material indicates its potential to become a highly porous structure. Although this carbonized material was not subjected to any activation process for the pores exposure, it is possible to state that it showed good results, in comparison to the commercial activated carbon. After the major carbon composition, the oxygen presents the higher contents. It must be noticed that the CCC presented a greater value of oxygen (12.43%) when compared to the CAC (12.43%). The higher oxygen levels may become an advantage for the CCC, since the oxygenated groups (e.g. lactones, hydroxyl, carbonyl, carboxyl, etc) that may interact with different adsorbates.

According to the extensive review performed by Shafeeyan, Wan Daud, Houshmand, & Shamiri (2010), the concentration of oxygen on an adsorbent's surface strongly impacts on the adsorption performance of the carbon.

The other inorganic elements, such as Mg and K are common macronutrients required by the plant. After the carbonization process, such elements can be observed in the form of oxides onto the carbon's surface,

which contributes to the alkaline character of the carbon. In addition, it is possible that the potassium and magnesium, in the form of nitrogen oxides, participate in the neutralization reactions of the free fatty acids present in the frying residual oil.

Table 3. Elemental composition, moisture (X) and ash (Ash) contents of the adsorbents (% m m⁻¹).

Samples	C (%)	O (%)	Mg (%)	Si (%)	Cl (%)	K (%)	X (%)	Ash (%)
CC	54.29	43.28	ND	ND	0.08	2.37	7.24	1.95
CCC	85.58	12.43	0.17	0.21	0.35	1.40	5.35	5.10
CAC	94.04	5.58	0.13	0.18	ND	ND	5.67	13.30

Chlorine is a micronutrient that plays a key role in the osmotic balance in the plants and also participates as an enzymatic cofactor in the photosystem II (PS II) in the water photolysis and O₂ liberation in the photosynthesis. Despite the fact that Si is not traditionally associated as an essential nutrient for plants, recently it has been recognized as an important element in the defence mechanism under stress conditions and in the resistance to fungus contamination. Monocotyledonous plants are particularly, silicon accumulators. Not only Si but also Mg may be present in the form of ash in the samples, as found by Kikuchi, Qian, Machida and Tatsumoto (2006).

In the analysis of pH_{PZC} (see Figure S3) both samples showed basic character surface (CCC: 8.61 and CAC: 8.04), which is a desirable feature for the adsorbents, since the goal of this project is to promote the adsorption of free fatty acids molecules present in the frying residual oil, reducing their acidity index.

Although the difference was small, it was noted that the CCC presented even a more basic surface than CAC. This basicity is given as a function of each material's composition, *i.e.* of the functional groups present in their superficial structures. Thus, it can be suggested that CCC has greater affinity for free fatty acids than CAC.

Through the infrared analysis (Figure S4) samples of RFO and RFOT with each adsorbent, it is noted that both spectra exhibit findings of typical characteristics of esters molecules, indicated by the bond C = O (1,630 to 1,810 cm⁻¹) and bond C (1,020 to 1,250 cm⁻¹). For RFO, there is a peak in 3,647 cm⁻¹ which is no longer seen in samples of RFOT (CAC and CCC). It can be attributed to the hydrogen bonds, carboxylic acids or water possibly present in the material. Its disappearance may indicate that there was the elimination of fatty acids during the process (Dovbeshko, Gridina, Kruglova, & Pashchuk, 2000; Pavia et al., 2010, Smidt & Meissl, 2007).

In 1,581 cm⁻¹, a small peak is seen in the sample of ORT and ceases to exist in oil samples treated with both adsorbents. It can be related to the presence of NH₂ groups of potential protein compounds present in RFO. In the case of the presence of amines, another band appears around 800 cm⁻¹, which refers to the creases N-H outside the plan. The absence of these peaks in samples of RFOT can be attributed to the elimination of this compound in the acidity removal by some form of interaction with the adsorbents (Pavia et al., 2010).

Molecular dynamics simulation

The RFO molecules dimensions determined in fatty acid composition were estimated, initially, by the minimizing energy MMFF94 method (Table 4), and subsequently by the HARTREE-FOCK method (HF). However, for this method, only the oleic acid was used for the analysis, in which despite of being the second most abundant in the sample, was easily obtained the most for testing in the laboratory.

Table 4. Fatty acid composition of the RFO and the fatty acids dimensions estimated by computational method MMFF94.

Fatty acids		AR (%)	Molecular dimensions	
			d _{long} ^a (Å)	d _{av} ^b (Å)
C14:0	Myristic	0.22	19.4	2.2
C16:0	Palmitic	12.05	22.0	2.2
C18:0	Stearic	4.33	24.1	2.2
C18:1	Oleic	32.20	14.5	7.6
C18:2	Linoleic	43.26	14.2	6.8
C18:3	Linolenic	3.77	10.8	8.7
C20:0	Arachidonic	0.34	26.6	2.2

AR: relative area. ^aLongitudinal diameter (Å); ^bAverage diameter (Å).

Evaluating the results obtained for the first simulation method, in comparison with the average pores diameter (Table 2), it is verified that, apparently, it is possible that the FFAs diffused inside the CCC pores as the largest dimension observed was 26.6 Å to the linear FFAs (for example C20:0), and for the non-linear

(unsaturated) approximately $14.5 \times 7.6 \text{ \AA}$ (Oleic – C18:1) and $14.2 \times 6.8 \text{ \AA}$ (linoleic – C18:2) that, apropos, are those that appear in larger quantity (approximately 75 %).

However, when assessing the oleic acid dimensions and molecular structure through the HARTREE-FOCK computational method, which also considers the electron cloud, a bigger molecule size was observed.

In Figure 3(a) it is possible to check the three-dimensional structure of the oleic acid molecule (octadec-9-enoic acid) with its *cis* preferential conformation, total height of 10.8 \AA and total length of 29.7 \AA , considering the electronic “cloud” throughout the molecule.

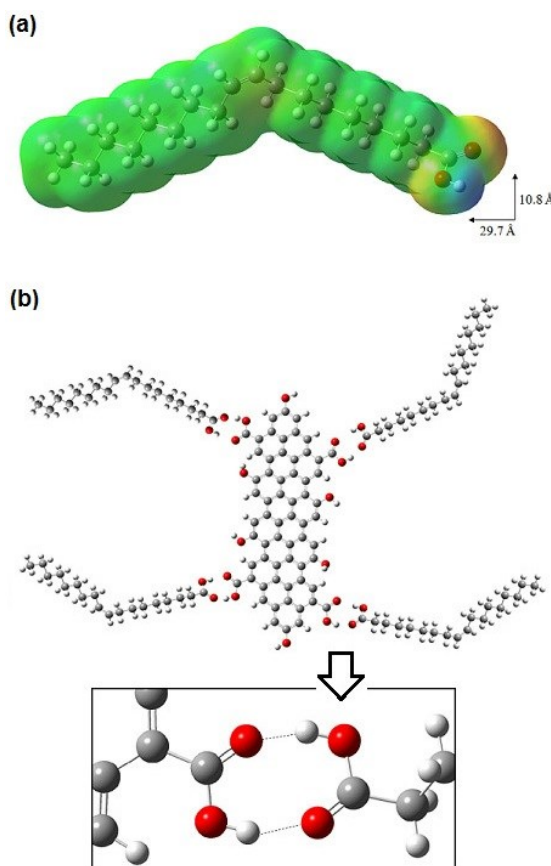


Figure 3. Molecular dynamics simulation: (a) Oleic acid 3-D structure and electronic cloud (theoretical); and (b) Possible interaction mechanism (H-Bond) between the oleic acid molecules (*i.e.* FFA) and the functional groups (active sites) on the adsorbent surface.

Comparing these dimensions with those observed by BET and BJH methods (see Table 2) to the average diameter of the adsorbent pores, it seems that, in the case of CCC and the CAC, with pore diameters of 27.50 \AA and 25.26 \AA , respectively, this oleic acid molecule could not easily and completely diffuse into the pores due to steric factors, as they are smaller than the FFA molecule.

Figure 3(b) implies, by the same method of semi-empirical analysis, a generic surface of an activated carbon, with its active functional groups interacting with those of the FFA molecule. Even though the FFA molecules cannot enter fully into the activated carbon pores, remaining only on their surfaces, it is possible that these superficial interactions are responsible for the removal process of free acidity in the frying residual oil. In addition to the weak forces of Van der Waals interactions, hydrogen bonds type (2.8 \AA) are indicated, characterizing a moderate force formed between a hydrogen atom of a an FFA molecule with one atom of oxygen of an active group present in the activated carbon, and vice versa. In the case of the molecule that can partially enter into the pore structure, it can also be suggested, that this part which diffuses into the internal pores may interact with the functional groups present in the interior of the pore in the same way as they interacted with more accessible groups onto the adsorbent's surface.

Adsorption experiments – RCCD: Operational variables optimization

In the adsorption tests the proportion in mass of adsorbate/adsorbent ranged from 0.09 to 0.15 considering the smallest and the largest used mass of adsorbent; the contact time was 6 h for all the tests. The average results were expressed in terms of RA percentage. Tests are shown in Figure 4.

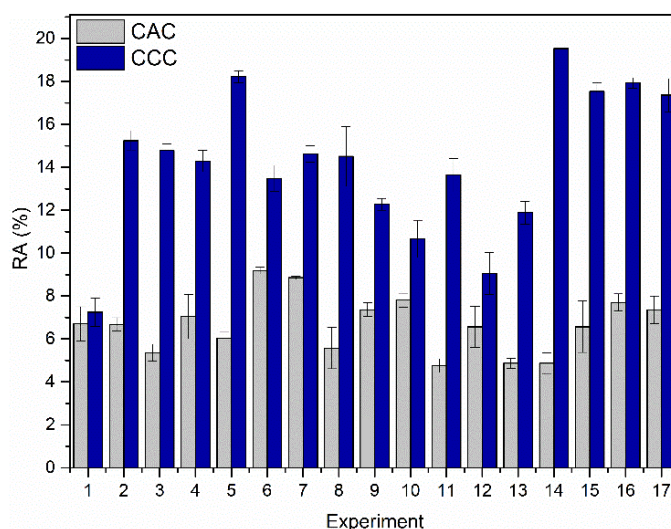


Figure 4. Experimental results of the adsorption assays by the RCCD for the CAC and CCC.

Considering that the initial acidity index of RFO was $3.84 \text{ mg KOH g}^{-1}$, for the CCC, the largest percentage of acidity reduction was obtained in the Experiment 14 ($T = 20^\circ\text{C}$; $A = 175 \text{ rpm}$; $M = 5 \text{ g}$), with a maximum reduction of 19.53 %, reaching an acid index of $3.09 \text{ mg KOH g}^{-1}$ of oil. Concerning CAC, the best result was obtained in the Experiment 6 ($T = 23^\circ\text{C}$; $A = 145 \text{ rpm}$; $M = 4.6 \text{ g}$), achieving a less significant reduction compared to CCC, reaching only 9.19 %, which is equivalent to an acid index of $3.34 \text{ mg KOH g}^{-1}$ of oil.

The experimental results of the RCCD were statistically analysed, and it was verified that the proposed model was valid for both adsorbents, which proved to be significant at 95% level of confidence ($p < 0.05$).

The Pareto charts of samples of CAC and CCC are presented in Figure S5 and Figure S6. In the case of CAC (Figure S5) it can be noticed that the quadratic terms of the factors Adsorbent Mass (M) and Agitation (A), as well as the linear interaction between the Agitation and Adsorbent Mass, were statistically significant ($p\text{-value} < 0.05$) and they showed negative values, evidencing its adverse influence over de acidity reduction, leaving the process at a disadvantage.

This behaviour can be observed in the CAC response surfaces (Figure 5), in which the entire response is favoured for higher values of adsorbent mass and temperature. The agitation also showed a lesser influence. However, one may notice that the performance of CAC performance over the acidity reduction was not strongly enhanced by the operational variables (at least in the studied range), in which only a slight increase and a tendency was observed. Also, in Figure 5, one may notice the second order equation, which was statistically valid given the ANOVA (Regression).

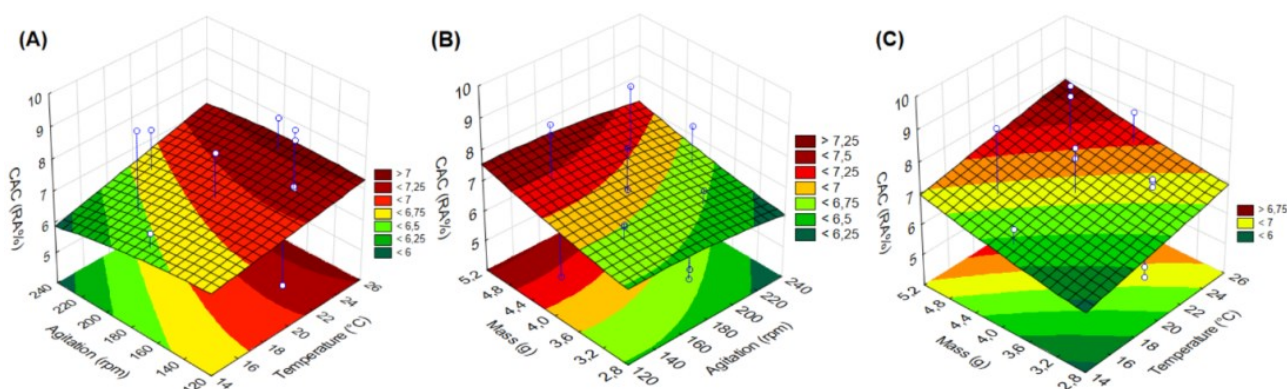


Figure 5. Response surfaces for RA% by the CAC for the interaction of independent variables: (A) Temperature (T) \times Agitation (A); (B) Adsorbent Mass (M) \times Agitation (A); and (C) Adsorbent Mass (M) \times Temperature (T); Equation (Real values): $RA_{CAC}(\%) = -245.865 + 12.325T - 0.180T^2 + 0.966A - 0.002A^2 + 25.105M - 0.526M^2 - 0.0117A - 0.786TM - 0.016AM$; ANOVA (Significant terms): Mass (Q): $F_{\text{calc}}(16.35354)$, $p\text{-value}(0.000471)$; Agitation (Q): $F_{\text{calc}}(10.60848)$, $p\text{-value}(0.003344)$; $T \times A$ interaction: $F_{\text{calc}}(7.36902)$, $p\text{-value}(0.012095)$. ANOVA (Regression): $F_{\text{calc}}(3.83104)$, $F_{\text{tab}}(9;24;5\%) (2.3002)$ – Model is statistically valid ($F_{\text{calc}} > F_{\text{tab}}$).

Regarding CAC (Figure 5), possibly the temperature increase may have provided greater interaction (collisions) among the adsorbate molecules (collisions), facilitating the fatty acids access to the mesopores or

the adsorbent active sites. In contrast, the increase in agitation of the reaction medium may have caused the molecules displacement already adsorbed. Thus, agitation lower than or equal to 145 rpm would have been enough to promote the movement necessary for the molecules to reach the adsorption sites.

In relation to the CCC data, from the Pareto diagram (see Figure S6) the significant values (*i.e.* p -value < 0.05) were the variables: Agitation (quadratic term), Temperature (quadratic term) and Adsorbent Mass (linear term). The factors A^2 and T^2 , showed negative values, whereas the M factor had a positive value indicating that its increase provides higher acidity reduction levels. Also, the linear interaction $T \times M$ presented a significant and negative effect over the response. An interaction between two variables generates a secondary effect that characterizes the synergism between the two factors. The surface responses for the RCCD for the influence of the operational variables over the acidity reduction for the CCC are presented in Figure 6.

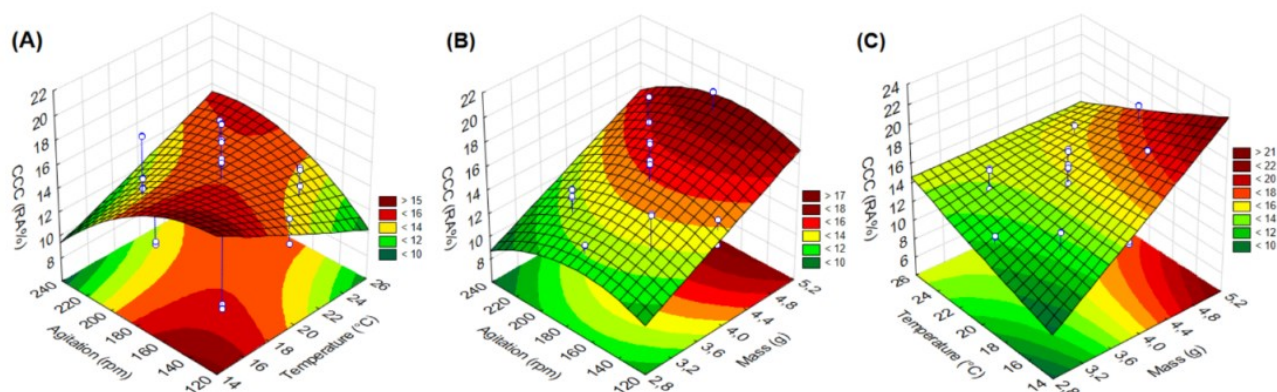


Figure 6. Response surfaces for RA% by the CCC for the interaction of independent variables: (A) Temperature (T) \times Agitation (A); (B) Adsorbent Mass (M) \times Agitation (A); and (C) Adsorbent Mass (M) \times Temperature (T); Equation (Real values): $RA_{CCC}(\%) = -245.865 + 12.325T - 0.180T^2 + 0.966A - 0.002A^2 + 25.105M - 0.526M^2 - 0.0117A - 0.786TM - 0.016AM$; ANOVA (Significant terms): Agitation[Q]: $F_{\text{calc}}(18.14610)$, p -value (0.000273); Temperature[Q]: $F_{\text{calc}}(15.51603)$, p -value (0.000615); Mass [L]: $F_{\text{calc}}(13.79557)$, p -value (0.001081); Interaction T \times M: $F_{\text{calc}}(6.75225)$, p -value (0.015757). ANOVA (Regression): $F_{\text{calc}}(6.4489)$, $F_{\text{tab}}(9;24;5\%) (2.3002)$ – Model statistically valid ($F_{\text{calc}} > F_{\text{tab}}$).

Overall, one may notice that the higher levels of adsorbent mass lead to an increase on the acidity removal, what is expected since a higher number of available sites for the FFA is provided. In contrast, the temperature effect (quadratic as well as interaction terms) impairs the acidity removal. This behaviour is probably related with the strong influence of the temperature over the oil properties (*e.g.* viscosity) as well as over its intermolecular interactions, namely, the H-bonds forces between the FFAs and the adsorbent's surface sites (see Figure 3b) can be weakened with the temperature increase.

It could be expected that, at higher temperatures the removal FFA process would be facilitated due to a higher diffusivity of the FFA molecules inside the pores (*i.e.* in the case that diffusional mechanism prevailed). However, the best RA results were observed at lower temperatures. Therefore, the adsorption process is probably governed by the adsorbent-adsorbate affinity rather than diffusional resistances. This behaviour is in accordance with molecular dimensions and pore size distribution as discussed in the previous sections.

Adsorption kinetics

In the best conditions obtained in the RCCD, namely, for CAC ($T = 23^\circ\text{C}$; $M = 4.6$ g; and $A = 145$ rpm) and for CCC ($T = 20^\circ\text{C}$; $M = 5.0$ g; and $A = 175$ rpm), adsorption kinetics experiments were performed as presented in Figure S7) By analyzing the adsorption kinetics for the CCC, within the first 30 min of contact between the CCC and RFO, an acidity reduction of 22.34% was observed. However, the equilibrium was only achieved after 4 h of contact, wherein 38.44% of RA was observed. It must be highlighted that this is a favourable kinetics considering that the oil presents a high viscosity, that impairs the diffusional processes in the fluid phase as well as inside the pores. For the CAC a smaller and almost constant percentage reduction was verified, in which the equilibrium was observed within 1 h of contact, however the RA was only 6.57%, *i.e.* a slight variation along the experiment.

Note: The equilibrium time of the kinetics data was confirmed by ANOVA and by the post-hoc tests, namely, Tukey's and Fischer's multiple comparison of means. For the CCC adsorbent, the effect of time

variable was considered significant over the RA(%) response, for a 5% of significance level (p -value = 6.9104×10^{-9}), whereas for the CAC there was no significant difference between the values. Also, for CCC kinetic data, both Tukey and Fischer post-hoc analysis evidenced that there were no significant differences between the RA values after 4h of contact time, confirming that equilibrium time was reached within 4h of experiment. Furthermore, the first derivative was applied to kinetic data wherein the inclination for times higher than 4h were very close to zero, therefore, confirming the stability was achieved after 4h.

In the beginning of the process, an elevated rate of FFA removal was observed due to the promptly available external active sites available. Subsequently, less accessible sites inside the pore structure took place, however, in a slower way.

From the moment in which the molecules begin to be sorbed, the sorption speed decreases, since the driving force reduces and only internal active sites are still unoccupied for the adsorbate molecules (Sud, Mahajan, & Kaur, 2008; Weber & Smith, 1987).

In mesoporous materials, adsorption takes place through the pores of wider diameter, that facilitates the passage of adsorbate molecules inside the structure, a factor that may explain the speed in which the process occurs. In this sense, by observing in the pore size distribution (see Figure S2), one may notice that the CAC presents a wider distribution of pores ranging majorly from 20 to 80 Å, but also showing wider pores up to 260 Å. In contrast, the CCC presented a very narrow pore structure (20 to 40 Å), showing no larger pores in its distribution. By confronting these results with the acidity removal (see Figure 4 and S6) one may notice that the CAC macropore structure was not efficient to promote the FFA removal.

Despite the larger pores commonly known as access pores may favor the kinetics for the process, for our system that was not observed. In fact, a jeopardizing effect was observed for the larger pores present in the CAC. Such behavior, may be related to the competition for the active sites between the FFA molecules (target) and other larger molecules present in the RFO, such as monoacylglycerols (MAG), diacylglycerols (DAG) and the triacylglycerols (TAG) which may have been adsorbed preferentially before FFA, hence causing an adverse effect to the FFA removal.

In other words, since the CCC present a very defined and narrow pore size (20 to 40 Å), the CCC acted similarly to a molecular sieve, wherein only FFA molecules could diffuse into the porous structure and achieve the internal active sites (since FFA molecules presented molecular sizes lower than 40 Å – see Table 4), explaining its best performance when compared to CAC adsorbent.

Despite the textural and porous structure influence over the acidity reduction, one may notice that the affinity can be a major factor for the FFA removal. Hence, given the greater presence of oxygen-containing groups as observed in the EDS elemental analysis (see Table 4), a higher affinity between the adsorbent and the adsorbate is expected (Shafeeyan et al., 2010), as observed for the CCC.

Also, in this process, neutralization reactions may have occurred, given the presence of basic groups on the adsorbents surface (as discussed in the pH_{PZC} results – see Figure S3) mainly in the CCC samples, where there was a greater acidity reduction.

Generally, an adsorption process kinetics comprehends a multiple-resistance sequential steps, which may include: (i) external resistance (film diffusion); (ii) internal resistance (intraparticle diffusion) and (iii) adsorption on the sites (Neves et al., 2018; Ruthven, 1984). Based on the textural properties along with the molecular geometry simulations for this study, a mechanism involved in the FFA retention onto the CCC adsorbent can be proposed. Given the pore sizes, the internal diffusion is plausible, hence it may control the overall mass transfer process. Also, oxygenated functional groups on the adsorbent's surface may act as active sites for the FFA molecules, which can interact mainly by H-bonds (even though other intermolecular interactions such as Van der Waals forces may also take place between the apolar part of the FFA molecule – see Figure 3a – and the apolar regions of the carbons

Adsorbent mass evaluation

After the definition of the equilibrium time (4h) in the kinetics experiments, the evaluation of the adsorbent mass was performed, as presented in Figure S8 it should be noted that there was a substantial difference among the percentages of acidity reduction comparing the CAC and CCC adsorbents. In general, CCC acidity removal performances were superior for all adsorbent mass studied confirming its higher affinity to the FFA as previously discussed.

Based on ANOVA and multiple comparison of means (Tukey and Fischer tests), the adsorbent mass was identified as a significant variable for both adsorbents (ANOVA at 5% confidence level): CAC (p -value =

2.2074×10^{-12}) and CCC (p -value = 1.1408×10^{-10}). The results of Tukey post-hoc comparison of means showed that for CAC there were no significant difference between the adsorbent mass values higher than 7, whereas for CCC the values of 4 to 10 g were statistically equal.

In summary, it was observed that CCC presented a higher acidity reduction achieving $34.70\% \pm 1.43\%$ for adsorbent mass values between 4 and 10 g, whereas CAC achieved $14.35\% \pm 0.28\%$ of RA for adsorbent mass values between 7 and 10 g. Therefore, it is possible to infer that, in these conditions, the FFA removal process became stable with 4 g of CCC adsorbent (resulting a mass ratio adsorbent: oil of 12.1% – *i.e.* adsorbent dosage), in a way that higher amounts of adsorbent would not provide higher FFA removal levels.

This disparity in the acidity reduction maybe related to the composition of each adsorbent and, consequently, to the adsorbent-adsorbate affinity (as discussed in the previous sections), mainly in what refers to the number of active sites, or even to greater availability of the contact surface. It must be highlighted that the steric effects of the adsorbed compounds, related to the pore's distribution and to the RFO molecules diameter played a key role in the acidity removal in this study, impacting on the competition for the active sites between FFA and higher molecules for the CAC adsorbent. In contrast, given the narrow pore size distribution presented by the CCC adsorbent, the removal of FFA was favoured through a molecular sieving effect inside the pores (*i.e.* the CCC presented a desirable selectivity for the FFA target adsorbate).

Impregnated adsorbent calorific potential

In the proposed adsorption process, a process residue is generated, namely, the activated carbon impregnated with the frying residual oil. Aiming to evaluate its potential to energetic purposes as solid fuel for the thermal energy generation, its calorific power was analysed. Specifically, for the CCC impregnated with RFO, a value of $31,933 \text{ J g}^{-1}$ was found, which represents a high value, enough for the present purpose.

In the literature, the values observed for soybean oil, in line with most of the vegetable oil, varied from 34,000 to 39,400 J g^{-1} (Martini, Delalibera, & Weirich Neto, 2012), while the corn cob exhibited approximately 15,000 to 17,000 J g^{-1} .

The value obtained in this mixture may be the result of the interaction among the characteristics of each component, or only the predominance of frying residual oil. In any case, these results show that the residue obtained on the use of carbonized corn cobs as adsorbent in the free acidity removal of frying residual oil can be used (*e.g.* pellets) in the burning in boilers and furnaces for thermal energy generation.

Conclusion

In general, carbonization process of the corn cobs led to enhanced textural properties, which allowed the FFA diffusion into the CCC, as well as oxygen functional groups, providing affinity to the FFA. The temperature showed an adverse effect over the FFA removal, which is probably related to the weakening of the H-bonds between the carboxylic groups of the FFA and oxygenated groups onto the adsorbent's surface. The kinetics experiment evidenced a favorable process reaching an equilibrium time after 4h, wherein 4 g was enough to achieve the maximum acidity removal. The material can be further used for energetic purposes.

Symbols

R^2 – determination coefficient
 p – p -value
 p/p_0 – relative pressure

Abbreviations

AI – Acidity Index.
RA – Acidity Reduction.
A – Agitation Speed.
BJH – Barret, Joyner and Halenda (1951) method.
CAC – Commercial Activated Carbon.
CCC – Carbonized Corn Cob.
CC – Corn Cob in natura.
DAG – Diacylglycerols.

FAO – Food and Agriculture Organization of the United Nations.
 FFA – Free Fatty Acids.
 RFO – Residual frying oil.
 pH_{PCZ} – Hydrogen ion potential at the zero-charge point.
 M – Adsorbent Mass.
 MAG – Monoacylglycerols.
 BET – Nitrogen Physisorption method (Brunauer, Emmett, & Teller, 1938).
 RCCD – Rotational Central Composite Design.
 SEM – Scanning Electron Microscopy.
 T – Temperature.
 TAG – Triacylglycerols.

References

- American Oil Chemists' Society. (2009). *AOCS CD 3D-63: Sampling and analysis of commercial fats and oils*. Urbana, IL: Author.
- Ali, R. F. M., & El Anany, A. M. (2014). Recovery of used frying sunflower oil with sugar cane industry waste and hot water. *Journal of Food Science and Technology*, 51(11), 3002-3013. doi: 10.1007/s13197-012-0832-7
- Barrett, E. P., Joyner, L. G., & Halenda, P. P. (1951). The determination of pore volume and area distributions in porous substances. I. Computations from nitrogen isotherms. *Journal of the American Chemical Society*, 73(1), 373-380. doi: 10.1021/ja01145a126
- Berrios, M., & Skelton, R. L. (2008). Comparison of purification methods for biodiesel. *Chemical Engineering Journal*, 144(3), 459-465. doi: 10.1016/j.cej.2008.07.019
- Bonassa, G., Schneider, L. T., Alves, H. J., Meier, T. R. W., Frigo, E. P., & Teleken, J. G. (2016). Sugarcane bagasse ash for waste cooking oil treatment applications. *Journal of Environmental Chemical Engineering*, 4(4), 4091-4099. doi: 10.1016/j.jece.2016.09.017
- Brunauer, S., Emmett, P. H., & Teller, E. (1938). Adsorption of gases in multimolecular layers, *Journal of the American Chemical Society*, 60(2), 309-319. doi: 10.1021/ja01269a023
- Cai, Z. -Z., Wang, Y., Teng, Y. -L., Chong, K. -M., Wang, J. -W., Zhang, J. -W., & Yang, D. -P. (2015). A two-step biodiesel production process from waste cooking oil via recycling crude glycerol esterification catalyzed by alkali catalyst. *Fuel Processing Technology*, 137, 186-193. doi: 10.1016/j.fuproc.2015.04.017
- Casallas, I. D., Carvajal, E., Mahecha, E., Castrillon, C., Gomez, H., Lopez, C., & Malagon-Romero, D. (2018). Pre-treatment of waste cooking oil for biodiesel production. *Chemical Engineering Transactions*, 65, 385-390. doi: 10.3303/CET1865065
- Diya'uddeen, B. H., Abdul Aziz, A. R., Daud, W. M. A. W., & Chakrabarti, M. H. (2012). Performance evaluation of biodiesel from used domestic waste oil: A review. *Process Safety and Environmental Protection*, 90(3), 164-179. doi: 10.1016/j.psep.2012.02.005
- Dovbeshko, G. I., Gridina, N. Y., Kruglova, E. B., & Pashchuk, O. P. (2000). FTIR spectroscopy studies of nucleic acid damage. *Talanta*, 53(1), 233-246. doi: 10.1016/S0039-9140(00)00462-8
- European Committee for Standardization. (2003). *EN 14103: Fat and oil derivatives: Fatty Acid Methyl Esters (FAME): Determination of ester and linolenic acid methyl ester contents*. Brussels: Author.
- Fonseca, J. M., Cardozo-Filho, L., Teleken, J. G., Silva, C. (2018). Ethyl esters from waste oil: Reaction data of non-catalytic hydroesterification at pressurized conditions and purification with sugarcane bagasse ash. *Journal of Environmental Chemical Engineering*, 6(4), 4988-4996. doi: 10.1016/j.jece.2018.07.044
- Fonseca, J. M., Teleken, J. G., Almeida, V. C., Silva, C. (2019). Biodiesel from waste frying oils: Methods of production and purification. *Energy Conversion and Management*, 184, 205-218. doi: 10.1016/j.enconman.2019.01.061
- Food and Agriculture Organization of the United Nations. (2017). *Food outlook: Biannual report on global food markets*. Retrieved from <https://bit.ly/3lG2y5c>
- Freitas, F. B. A., Câmara, M. Y. F., & Martins, D. F. F. (2015). Determinação do PCZ de adsorventes naturais utilizados na remoção de contaminantes em soluções aquosas. *Blucher Chemistry Proceedings*, 3(1), 1-8. Retrieved from <https://bit.ly/32NMVRA>

- Gregg, S. J., & Sing, K. S. W. (1982). *Adsorption, surface area and porosity* (2nd ed.). Cambridge, MA: Academic Press.
- Gupta, V. K., & Suhas (2009). Application of low-cost adsorbents for dye removal: A review. *Journal of Environmental Manage*, 90(8), 2313-2342. doi: 10.1016/j.jenvman.2008.11.017
- Kikuchi, Y., Qian, Q., Machida, M., & Tatsumoto, H. (2006). Effect of ZnO loading to activated carbon on Pb (II) adsorption from aqueous solution. *Carbon*, 44(2), 195-202. doi: 10.1016/j.carbon.2005.07.040
- Liu, K., Lin, X., Yue, J., Li, X., Fang, X., Zhu, M., Lin, J., Qu, Y., & Xiao, L. (2010). High concentration ethanol production from corn cob residues by fed-batch strategy. *Bioresource Technology*, 101(13), 4952-4958. doi: 10.1016/j.biortech.2009.11.013
- Lopes, C. W., Bertella, F., Pergher, S. B. C., Finger, P. H., Dallago, R. M., & Penha, F. G. (2013). Síntese e caracterização de carvões ativados derivados do sabugo de milho. *Perspectiva*, 37(139), 27-35. Recuperado em 20 jan. 2017 de <https://bitlybr.com/8LKldA>
- Maddikeri, G. L., Pandit, A. B., & Gogate, P. R. (2012). Intensification approaches for biodiesel synthesis from waste cooking oil: A review. *Industrial & Engineering Chemistry Research*, 51(45), 14610-14628. doi: 10.1021/ie301675j
- Manique, M. C., Faccini, C. S., Onorevoli, B., Benvenuti, E. V., & Caramão, E. B. (2012). Rice husk ash as an adsorbent for purifying biodiesel from waste frying oil. *Fuel*, 92(1), 56-61. doi: 10.1016/j.fuel.2011.07.024
- Martini, J., Delalibera, H. C., & Weirich Neto, P. H. (2012). Consumption of soybean oil preheated by diesel engine. *Revista Brasileira de Agrociência*, 18(2-4), 213-220.
- Miyashiro, C. S., Bonassa, G., Schneider, L. T., Parisotto, E. I. B., Alves, H. J., & Teleken, J. G. (2018). Evaluation of different adsorbents for acidity reduction in residual oil. *Environmental Technology*, 40(11), 1438-1454. doi: 10.1080/09593330.2017.1422807.
- Moruzzi, R. B., Lima, V. B., Colombo, R., Conceição, F. T., & Lanza, M. R. V. (2014). Remoção do ácido mefenâmico em água utilizando carvão ativado em pó, lama vermelha e oxidação com cloro. *Química Nova*, 37(10), 1594-1599. doi: 10.5935/0100-4042.20140269.
- Nascimento, R. F., Lima, A. C. A., Vidal, C. B., Melo, D. Q., & Raulino, G. S. C. (2014). *Adsorção: aspectos teóricos e aplicações ambientais*. Fortaleza, CE: Edições UFC.
- Neves, C. V., Scheufele, F. B., Nardino, A. P., Vieira, M. G. A., Silva, M. G. C., Módenes, A. N., & Borba, C. E. (2018). Phenomenological modeling of reactive dye adsorption onto fish scales surface in the presence of electrolyte and surfactant mixtures. *Environmental Technology*, 39(19), 2467-2483. doi: 10.1080/09593330.2017.1356876.
- Öztürk, T., & Esen, B. (2013). Physical and mechanical properties of some hybrid corn varieties. *International Journal of Agricultural and Biological Engineering*, 6(1), 111-116.
- Pavia, D. L., Lampman, G. M., Kriz, G. S., & Vyvyan, J. A. (2010). *Introdução à espectroscopia*. São Paulo, SP: Cengage Learning.
- Rocha Junior., J. G., Santos, M. D. R., Madeira, F. B., Rocha, S. F. L. S., Bauerfeldt, G. F., Silva, W. L. G., Salomão, A. A., & Tubino, M. (2019). Influence of fatty acid methyl ester composition, acid value, and water content on metallic copper corrosion caused by biodiesel. *Journal of Brazilian Chemical Society*, 30(8), 1751-1761. doi: 10.21577/0103-5053.20190078
- Ruthven, D. M. (1984). *Principles of adsorption and adsorption processes*. Hoboken, NJ: John Wiley & Sons.
- Schneider, L. T., Bonassa, G., Alves, H. J., Meier, T. R. W., Frigo, E. P., & Teleken, J. G. (2017). Use of rice husk in waste cooking oil pretreatment. *Environmental Technology*, 40(5), 594-604. doi: 10.1080/09593330.2017.1397772
- Shafeeyan, M. S., Wan Daud, W. M. A., Houshmand, A., & Shamiri, A. (2010). A review on surface modification of activated carbon for carbon dioxide. *Journal of Analytical and Applied Pyrolysis*, 89(2), 143-151. doi: 10.1016/j.jaap.2010.07.006
- Silva, F. A. M., Borges, M. F. M., & Ferreira, M. A. (1999). Methods for assessing the degree of lipid oxidation and antioxidant capacity. *Química Nova*, 22(1), 94-103. Retrieved from <https://bit.ly/3lC5a3V>.
- Silvério, H. A., Flauzino Neto, W. P., Dantas, N. O., & Pasquini, D. (2013). Extraction and characterization of cellulose nanocrystals from corn cob for application as reinforcing agent in nanocomposites. *Industrial Crops and Products*, 44, 427-436. doi: 10.1016/j.indcrop.2012.10.014

- Smidt, E., & Meissl, K. (2007). The applicability of Fourier transform infrared (FT-IR) spectroscopy in waste management. *Waste Management*, 27(2), 268-276. doi: 10.1016/j.wasman.2006.01.016
- Souza, N. E., Matsushita, M., & Visentainer, J. V. (2012). Ácidos graxos: estrutura, classificação, nutrição e saúde. *Arquivos da Apadec*, 2(2), 102-107. Retrieved from <https://bit.ly/3kxrREV>
- Sud, D., Mahajan, G., & Kaur M. P. (2008). Agricultural waste material as potential adsorbent for sequestering heavy metal ions from aqueous solutions – A review. *Bioresource Technology*, 99, 6017-6027. doi: 10.1016/j.biortech.2007.11.064
- Talebian-Kiakalaieh, A., Amin, N. A. S., & Mazaheri, H. (2013). A review on novel processes of biodiesel production from waste cooking oil. *Applied Energy*, 104, 683-710. doi: 10.1016/j.apenergy.2012.11.06.
- Teixeira, A. S. (1998). *Alimentos e alimentação dos animais*. Lavras, MG: UFLA-FAEPE.
- Ullah, Z., Bustam, M. A., & Man, Z. (2015). Biodiesel production from waste cooking oil by acidic ionic liquid as a catalyst. *Renewable Energy*, 77, 521-526. doi: 10.1016/j.renene.2014.12.040
- Vaughan, T., Seo, C. W., & Marshall, W. E. (2001). Removal of selected metal ions from aqueous solution using modified corncobs. *Bioresource Technology*, 78, 133-139. doi: 10.1016/S0960-8524(01)00007-4
- Vieitez, I., Callejas, N., Irigaray, B., Pinchak, Y., Merlinski, N., Jachmanián, I., & Grompone, M. A. (2014). Acid value, polar compounds and polymers as determinants of the efficient conversion of waste frying oil to biodiesel. *Journal of the American Oil Chemists' Society*, 91(4), 655-664. doi: 10.1007/s11746-013-2393-y
- Xia, W., & Budge, S. M. (2017). Techniques for the analysis of minor lipid oxidation products derived from triacylglycerols: epoxides, alcohols, and ketones. *Comprehensive Reviews in Food Science and Food Safety*, 16, 735-758. doi: 10.1111/1541-4337.12276
- Weber, W. J., & Smith, E. H. (1987). Simulation and design models for adsorption processes. *Environmental Science & Technology*, 21(11), 1040-1050. doi: 10.1021/es00164a002
- Yaakob, Z., Mohammad, M., Alherbawi, M., Alam, Z., & Sopian, K. (2013). Overview of the production of biodiesel from waste cooking oil. *Renewable and Sustainable Energy Reviews*, 18, 184-93. doi: 10.1016/j.rser.2012.10.016

Supplementary Material

Table S1. Specification of levels of the proposed experimental design (RCCD).

n	Factors (Independent variables)	-1.68	-1	0	1	1.68
X_1	Temperature (°C)	15	17	20	23	25
X_2	Adsorbent Mass (g)	3	3.40	4	4.60	5
X_3	Agitation Speed (rpm)	125	145	175	205	225

Table S2. Rotational Central Composite Design (RCCD) Matrix.

Tests	Coded Values			Real Values		
	X_1	X_2	X_3	T (°C)	A (rpm)	m (g)
1	-1	-1	-1	17	145	3.40
2	1	-1	-1	23	145	3.40
3	-1	1	-1	17	205	3.40
4	1	1	-1	23	205	3.40
5	-1	1	1	17	205	4.60
6	1	-1	1	23	145	4.60
7	-1	1	1	17	205	4.60
8	1	1	1	23	205	4.60
9	-1.68	0	0	15	175	4.00
10	1.68	0	0	25	175	4.00
11	0	-1.68	0	20	125	4.00
12	0	1.68	0	20	225	4.00
13	0	0	-1.68	20	175	3.00
14	0	0	1.68	20	175	5.00
15	0	0	0	20	175	4.00
16	0	0	0	20	175	4.00
17	0	0	0	20	175	4.00

Note: Full factorial design (1 to 8), axial points (9 to 14) and central points replicates (15 to 17). Analysis time: 6 h. Amount of oil in each sample: 33 g.

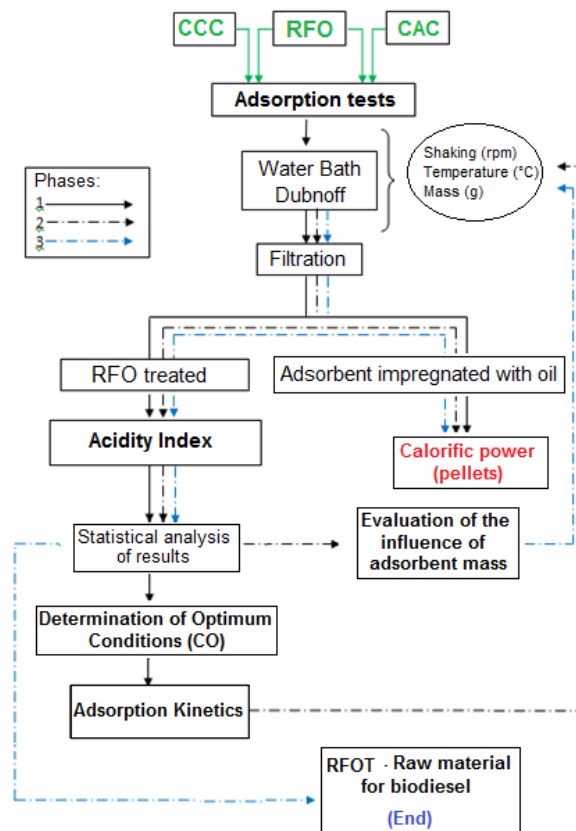


Figure S1. Flowchart of the procedure of the adsorption tests and statistical analysis of results.

Source: Author.

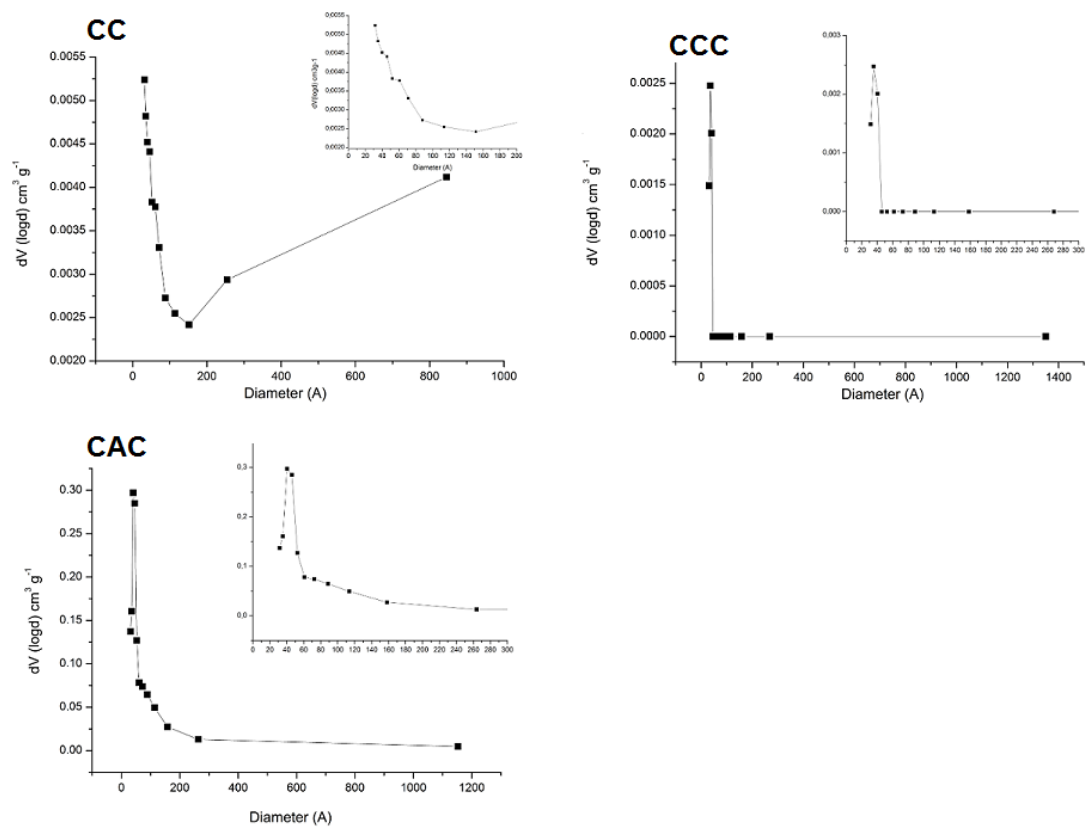


Figure S2. Pore size distribution of adsorbents: (CC) Corn Cobs; (CCC) Carbonized Corn Cobs; and (CAC) Commercial Activated Carbon.

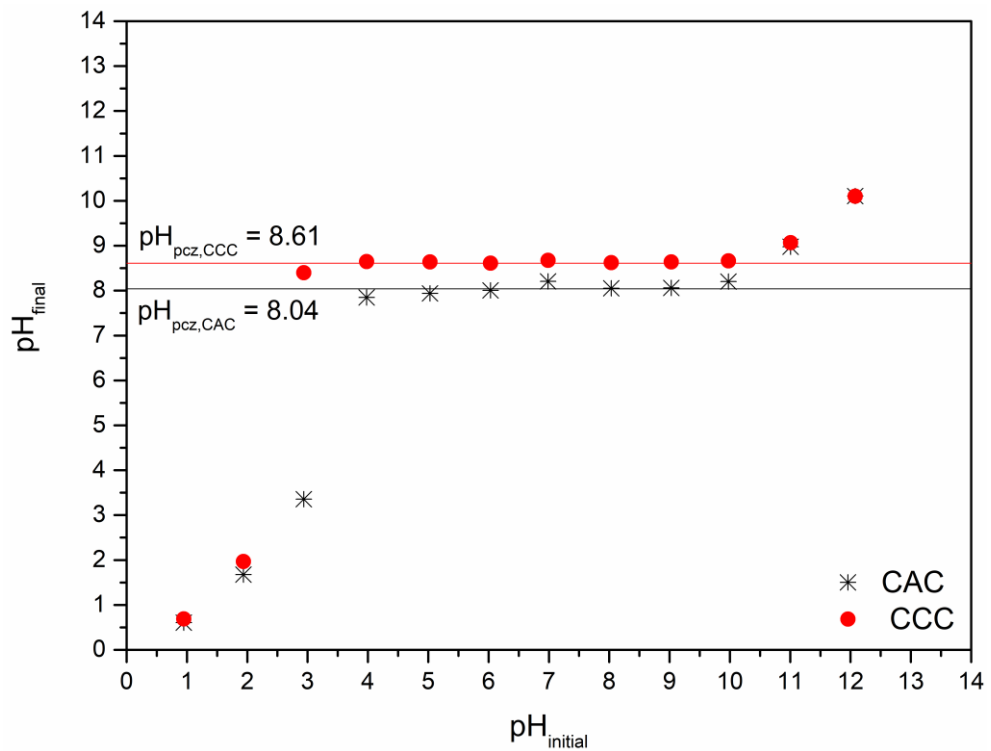


Figure S3. pH_{PCZ} analysis of samples of CCC and CAC adsorbent materials.

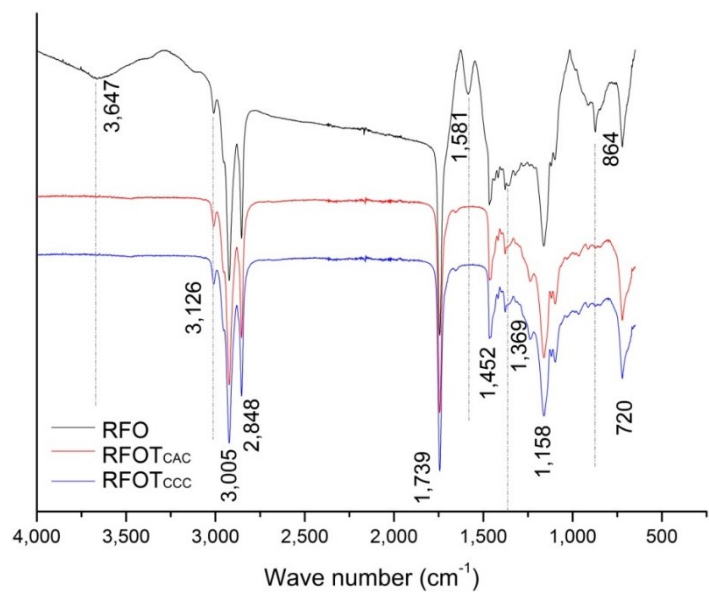


Figure S4. FTIR spectra of residual frying oil before (RFO) and after treatment with the CAC and CCC adsorbents.

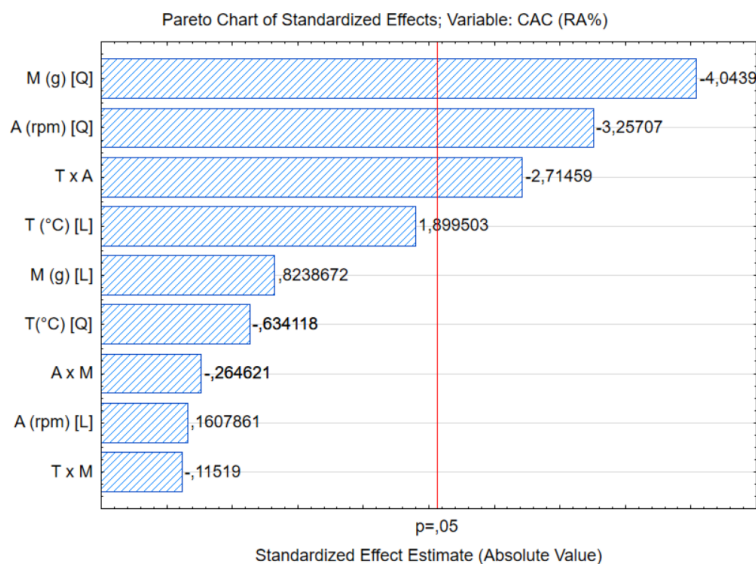


Figure S5. Pareto diagram obtained for the use of CAC over the acidity removal of the RFO.

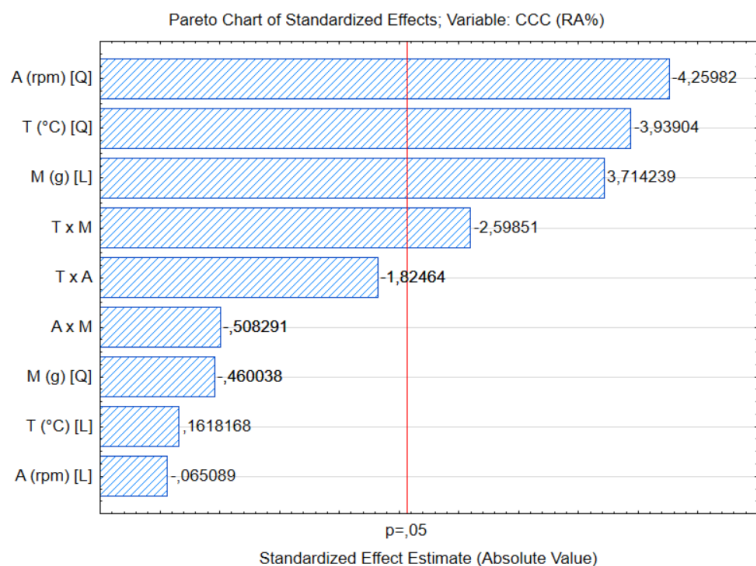


Figure S6. Pareto diagram obtained with the use of CCC over the acidity removal of the RFO.

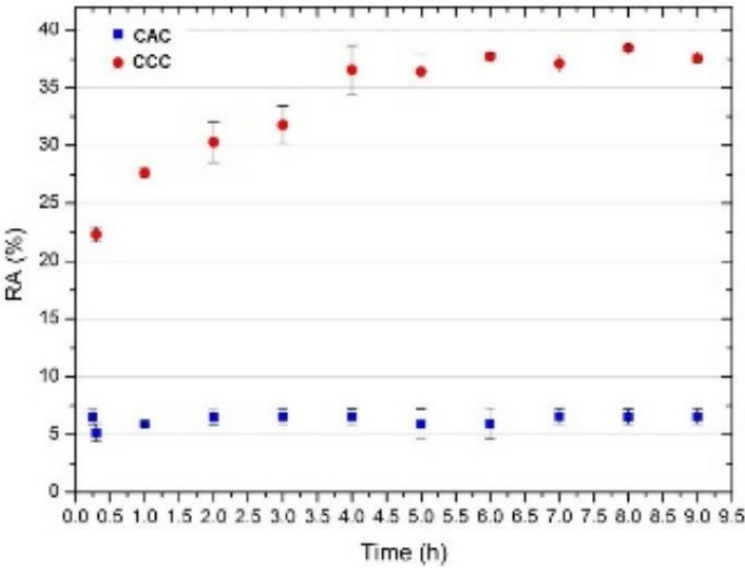


Figure S7. Adsorption kinetics of acidity removal of the RFO by the CAC and CCC adsorbents (in the best conditions of RCCD: CAC – T = 23°C; M = 4.6 g; and A = 145 rpm; CCC – T = 20°C; M = 5.0 g; and A = 175 rpm).

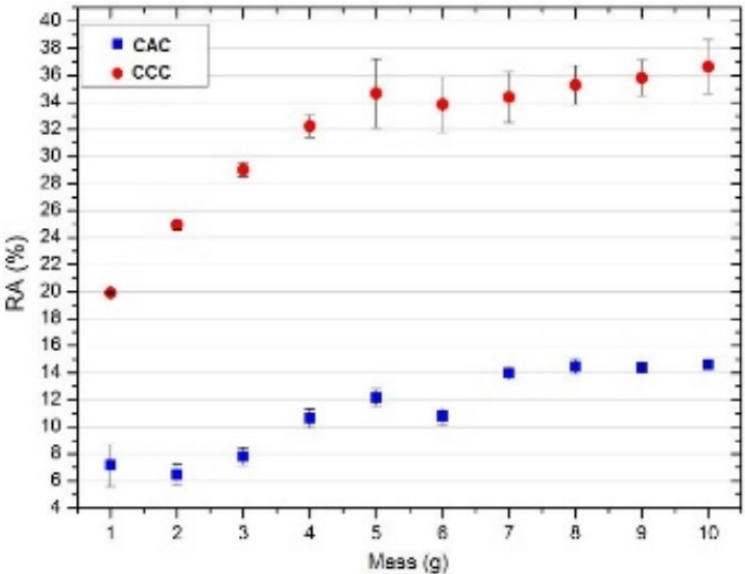


Figure S8. Influence of adsorbent mass over the acidity reduction by the CAC and CCC adsorbents in the best conditions obtained in the RCCD.